RSC Advances

PAPER

View Article Online
View Journal | View Issue

Cite this: *RSC Adv.*, 2014, **4**, 13919

Structures and properties of four coordination polymers constructed from 1,3-bis-(4-pyridyl)-propane and aromatic dicarboxylic acids†

Bo Xu,* Qing-Shan Liang, Lian-Tao Liu, Qi-Sheng Liu and Cun-Cheng Li*

Received 8th January 2014
Accepted 4th March 2014

DOI: 10.1039/c4ra00163j

www.rsc.org/advances

Four coordination polymers associated with 1,3-bis-(4-pyridyl) propane (bpp) and 5-methylisophthalic acid (H_2mip) or 5-nitroisophthalic acid (H_2nip) formulated as $[Zn(bpp)(mip)]_n$ (**1**), $[Co(bpp)(mip)]_n$ (**2**), $[Zn_2(bpp)_2(nip)_2]_n$ (**3**) and $[Co(bpp)(nip)(H_2O)]_n$ (**4**) have been synthesized under hydrothermal conditions. Single crystal analyses reveal that complex **1** presents a four-fold interpenetrating framework based on three-dimensional (3D) subunits with *dia* topology. Compound **2** has a 1D binuclear chain structure. Complex **3** shows 2D 4^4-sql layer structure packing in *ABAB* mode. Complex **4** exhibits a two-fold interpenetrating framework based on three-dimensional (3D) subunits with *dia* topology. These compounds have been characterized by infrared spectroscopy, elemental analysis, thermogravimetric analysis and powder X-ray diffraction. In addition, the photoluminescence of **1** and **3** and magnetic properties of **2** and **4** were investigated.

Introduction

Coordination polymers (CPs) are a class of hybrid material constructed from metal ions linked by organic ligands through coordination bonds. The rational design and construction of coordination polymers (CPs) have been receiving considerable attention over the past two decades not only because of the variety of their topological structures but also due to their excellent properties in many fields such as molecular separation, optics, catalysis and so on.[1–4] A large number of CPs with novel structures and fascinating properties have been obtained through different synthesis approach. But it is still a great challenge for us to effective control the construction of CPs with expected structure and property because too many factors as temperature, solvent system, counter ion and so on play important role on the assemble process.[5–7]

Design and speculation of the structure and property of CPs constructed from flexible ligands is much more difficult as flexible ligands usually show different configuration and various coordination modes when reaction with metal ions. We have long been focusing on the research of construction of CPs based on a flexible bipyridyl ligand *N*,*N*′-bis-(4-pyridyl-methyl) piperazine (bpmp) with a long spacer $-CH_2(C_4H_8N_2)CH_2-$ between the two pyridyl groups.[8] The rigidity and steric hindrance effect of the piperazine ring make it less flexible than the other flexible bipyridyl ligand as 1,3-bis-(4-pyridyl)-propane. As known, flexibility of the bipyridyl ligand has important influence on the resulting structures of the final products. Products with different topological structures may be obtained by rational design and tuning of the length and the flexibility of the bipyridyl ligands. Thus, based on our previous work, we now expand our research to the synthesis of CPs with mixed 1,3-bis-(4-pyridyl)-propane (bpp) ligand and aromatic dicarboxylic acids. 1,3-Bis-(4-pyridyl)-propane with a longer linker $-CH_2CH_2CH_2-$ between two pyridyl groups is more flexible and may show different configuration when coordinated to metal ions. But coordination mode of the bpp ligand is sole as it almost always holds the bidentate bridging mode. So two aromatic dicarboxylic acids including 5-nitroisophthalic acid and 5-methylisophthalic acid are involved as auxiliary ligands. These aromatic dicarboxylic acids are chosen as the auxiliary ligands mainly because of their various coordination modes on one hand. One the other hand, aromatic dicarboxylic acids usually deprotoned and act as anions when coordinating to metal cations and thus achieve charge balance without other anions as Cl^- or NO^{3-} get involved in the structure. Both of these two features may increase the opportunity for novel structures and interesting properties to some extent. This is also a current research focus and a large number of coordination compounds based on mixed N-coordinated ligand and polycarboxylate ligand system have been explored.[9–11] In this paper, we give a report of four compounds based on mixed 1,3-bis-(4-pyridyl)-propane (bpp) and different aromatic dicarboxylic acids including 5-methylisophthalic acid (H_2mip) and 5-

Key Laboratory of Chemical Sensing & Analysis in Universities of Shandong (University of Jinan), School of Chemistry and Chemical Engineering, University of Jinan, Jinan, Shandong, 250022, China. E-mail: chm_xub@ujn.edu.cn; chm_licc@ujn.edu.cn

† Electronic supplementary information (ESI) available: Figures showing PXRD patterns, TG curves and table showing selected bond lengths. CCDC 980158–980161 for the complexes **1–4**. For ESI and crystallographic data in CIF or other electronic format see DOI: 10.1039/c4ra00163j

nitroisophthalic acid (H_2nip), formulated as $[Zn(bpp)(mip)]_n$ (**1**), $[Co(bpp)(mip)]_n$ (**2**), $[Zn_2(bpp)_2(nip)_2]_n$ (**3**) and $[Co(bpp)(nip)(H_2O)]_n$ (**4**). We herein report the syntheses, structures, characterization and luminescent or magnetic properties of these compounds.

Experimental details

Materials and general methods

All commercially available reagents and starting materials were of reagent-grade quality and used without further purification. Elemental analyses (C, H, N) were carried out on an Elementar Vario EL III analyzer. Infrared (IR) spectra were recorded on Perkin-Elmer Spectrum One as KBr pellets in the range 4000–400 cm^{-1}. UV-visible absorption spectra were collected in Hitachi U-4100. Thermogravimetric analysis was recorded with a Perkin-Elmer Diamond TG/DTA instrument at a heating rate of 10 °C min^{-1} under nitrogen atmosphere. X-ray Powered diffraction (XRPD) patterns of the samples were recorded by an X-ray diffractometer (Rigaku D/Max 2200PC) with a graphite monochromator and CuKα radiation at room temperature while the voltage and electric current are held at 40 kV and 20 mA. Solid-state emission and excitation spectra are carried out on an Edinburgh FLS920 phosphorimeter equipped with a continuous Xe-900 xenon lamp and an nF900 ns flash lamp. Temperature-dependent magnetic measurements were carried out on a SQUID-MPMS-XL-7 magnetometer.

Synthesis of complexes 1–4

$[Zn(bpp)(mip)]_n$ 1. A mixture of $Zn(NO_3)_2\cdot 6H_2O$ (59.4 mg, 0.2 mmol), bpp (39.6 mg, 0.2 mmol), H_2mip (35.6 mg, 0.2 mmol) and NaOH (16.0 mg 0.4 mmol) in deionized water (10 mL), sealed in a 25 mL Teflon-lined stainless steel autoclave, and heated at 150 °C for 84 hours, then slowly cooled to room temperature during 12 hours. Colorless block crystals were recovered by filtration, washed by distilled water, and dried in air at ambient temperature. Yield: 67% (based on Zn). Calcd for $C_{22}H_{20}N_2O_4Zn$ (441.77): C 59.81, H 4.56, N 6.34; found: C 59.70, H 4.49, N 6.30. IR (KBr, cm^{-1}): 3434 (m, br), 3070 (w), 2927 (w), 1624 (vs), 1509 (m), 1430 (m), 1334 (s), 1236 (m), 1031 (m), 1022 (w), 829 (m), 773 (m), 730 (m).

$[Co(bpp)(mip)]_n$ 2. Compound **2** was prepared in the same way as that for **1** but using $Co(NO_3)_2\cdot 6H_2O$ (58.2 mg, 0.2 mmol) instead of $Zn(NO_3)_2\cdot 6H_2O$. Purple block crystals were recovered by filtration, washed by distilled water, and dried in air at ambient temperature. Yield: 63% (based on Co). Calcd for $C_{22}H_{20}N_2O_4Co$ (435.33): C 60.70, H 4.63, N 6.43; found: C 60.54, H 4.56, N 6.48. IR (KBr, cm^{-1}): 3369 (s, br), 2974 (w), 1616 (s), 1547 (m), 1427 (m), 1389 (s), 1224 (w), 1050 (m), 878 (w), 777 (w), 725 (m).

$[Zn_2(bpp)_2(nip)_2]_n$ 3. Compound **3** was prepared in the same way as that for **1** but using H_2nip (42.2 mg, 0.2 mmol) instead of H_2mip. Colorless block crystals were recovered by filtration, washed by distilled water, and dried in air at ambient temperature. Yield: 61% (based on Zn). Calcd for $C_{42}H_{34}N_6O_{12}Zn_2$ (945.49): C 53.35, H 3.62, N 8.89; found: C 53.24, H 3.53, N 8.77. IR (KBr, cm^{-1}): 3428 (w, br), 3100 (w), 2943 (w), 1643 (s), 1526 (m), 1434 (m), 1337 (s), 1236 (w), 1073 (m), 889 (w), 782 (w), 725 (m).

$[Co(bpp)(nip)(H_2O)]_n$ 4. Compound **4** was prepared in the same way as that for **3** but using $Co(NO_3)_2\cdot 6H_2O$ (58.2 mg, 0.2 mmol) instead of $Zn(NO_3)_2\cdot 6H_2O$. Red block crystals were recovered by filtration, washed by distilled water, and dried in air at ambient temperature. Yield: 65% (based on Co). Calcd for $C_{21}H_{19}N_3O_7Co$ (484.33): C 52.08, H 3.95, N 8.68; found: C 52.21, H 3.90, N 8.62. IR (KBr, cm^{-1}): 3410 (s, br), 3098 (m), 2955 (m), 1630 (s), 1534 (m), 1429 (m), 1367 (s), 1226 (w), 1072 (m), 820 (w), 786 (m), 732 (m).

Table 1 Crystal data and structure refinement parameters for compounds **1–4**

Complex	**1**	**2**	**3**	**4**
Empirical formula	$C_{22}H_{20}N_2O_4Zn$	$C_{22}H_{20}N_2O_4Co$	$C_{42}H_{34}N_6O_{12}Zn_2$	$C_{21}H_{19}N_3O_7Co$
Formula weight	441.77	435.33	945.49	484.33
Crystal system	Monoclinic	Triclinic	Triclinic	Monoclinic
Space group	$P2_1/n$	$P\bar{1}$	$P\bar{1}$	$C2/c$
a (Å)	11.0364(11)	8.9484(6)	9.5955(3)	14.4137(15)
b (Å)	11.3292(8)	10.1378(6)	14.7243(14)	18.2182(15)
c (Å)	15.9216(16)	11.8315(6)	14.8584(14)	16.6210(16)
α (deg.)	90	68.413(5)	67.778(9)	90
β (deg.)	103.696(9)	84.359(5)	85.961(5)	102.434(11)
γ (deg.)	90	78.184(5)	85.587(5)	90
V (Å^3)	1934.1(3)	976.58(10)	1935.7(3)	4262.2(7)
Z	4	2	2	8
D_{calc} (g cm^{-3})	1.517	1.480	1.622	1.510
F(000)	912	450	968	1992
Reflns collected/unique	10 107/3940	10 135/3996	17 261/7657	13 006/4359
μ (mm^{-1})	1.302	0.910	1.315	0.854
GOF on F^2	1.155	1.070	1.035	0.944
R_1,[a] ($I > 2\sigma(I)$)	0.0687	0.0386	0.0943	0.0768
wR_2[b] (all data)	0.1987	0.1024	0.2589	0.1844

[a] $R = \sum||F_o| - |F_c||/\sum|F_o|$. [b] $wR(F^2) = [\sum w(F_o^2 - F_c^2)^2/\sum w(F_o^2)^2]^{1/2}$.

Crystallographic details

Suitable single crystal with a approximate dimensions were mounted on a Xcalibur Eos Gemini diffractometer with graphite-monochromated Mo Kα (λ) 0.71073 Å radiation at room temperature. Data reduction was performed with the CrysAlisPro program.[12] Empirical absorption corrections were applied to the data using the SADABS program.[13] The structures were solved by direct methods and refined by the full-matrix least-squares on F^2 using the *SHELXTL-97* program.[14] All non-hydrogen atoms were refined with anisotropic displacement parameters. The positions of hydrogen atoms attached to carbon atoms were generated geometrically and refined with isotropic thermal parameters. Crystallographic data and structure determination summaries are listed in Table 1, and the selected bond lengths and angles for the complexes are listed in Table S1.† The topological analysis and some diagrams were produced using TOPOS program.[15]

Results and discussion

Crystal structure of 1

X-ray crystallographic analysis reveals that compound **1** crystallizes in the monoclinic space group $P2_1/n$. There are one Zn(II) ion, one mip^{2-} ligand and one bpp ligand in the asymmetric unit of complex **1**. The view of the local coordination environment of the Zn(II) center in **1** is illustrated in Fig. 1a. Each Zn(II) ion is tetrahedrally coordinated to two bpp ligands *via* the pyridyl N atoms (Zn1–N1 = 2.051(4) Å, Zn1–N2A = 2.046(4) Å), two mip^{2-} ligands *via* the carboxyl O atoms (Zn1–O1 = 1.961(3) Å, Zn1–O4A = 1.959(3) Å). Further insight into the structure of **1** found that the mip^{2-} ligand holds the η^1–η^1 bridging coordination mode as shown in Scheme 1a, while the bpp ligand acts as bidentate ligand with the dihedral angle between the two pyridyl groups is *ca.* 75.76° linking the Zn(II) ions to a 3D network. Topological analysis of **1** were carried out using the TOPOS program, and the result shows that complex **1** is a typically 3D fourfold interpenetrating diamond framework containing adamantanoid cages as shown in Fig. 1b. As known, large void in MOFs is usually occupied by guest molecules or filled through interpenetrating with other motifs. The capacious space of the adamantanoid cages in **1** causes four-fold interpenetration occurring and the final 3D fourfold interpenetrating diamond network is shown in Fig. 1c.

Crystal structure of 2

X-ray single crystal structure analysis reveals that the asymmetric unit of **2** consists of one crystallographically independent Co(II), one mip^{2-} anion, and one bpp ligand. As shown in Fig. 2a, the central Co(II) ion is six-coordinated by four oxygen atoms from two mip^{2-} anions and two nitrogen atoms from two bpp molecules. The coordination geometry of the Co(II) ion is a slightly distorted octahedron with the four oxygen atoms from two mip^{2-} anions define the equatorial positions and two nitrogen atoms from two bpp molecules occupied the axial positions. The mip^{2-} anion acts in a $\eta^2\mu_2$–η^2 coordination mode as shown in Scheme 1b with one of the two carboxylate groups adopts chelating coordination mode while the other one acts in a bidentate bridging mode linking two Co(II) ions to form binuclear structure. Meanwhile, the two Co(II) ions in the

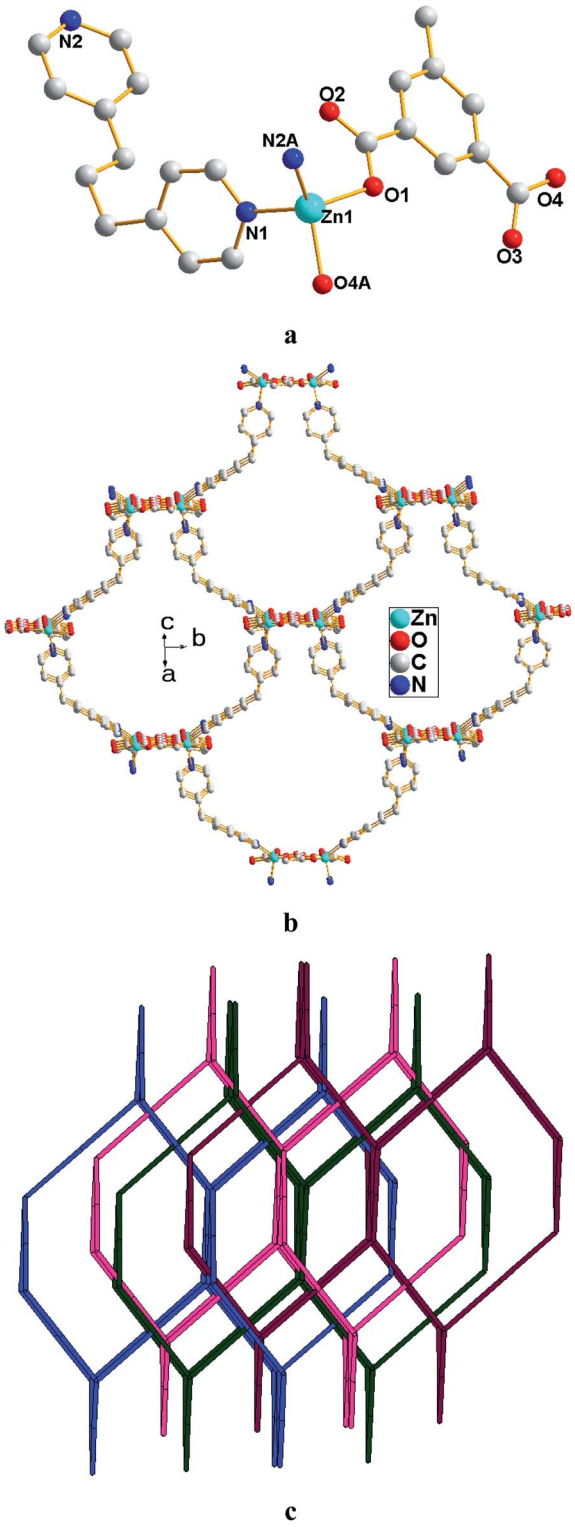

Fig. 1 (a) The coordination environment of Zn(II) ion in **1**; (b) view of the 3D *dia* network and (c) schematic illustration of the four-fold interpenetrating network in **1**.

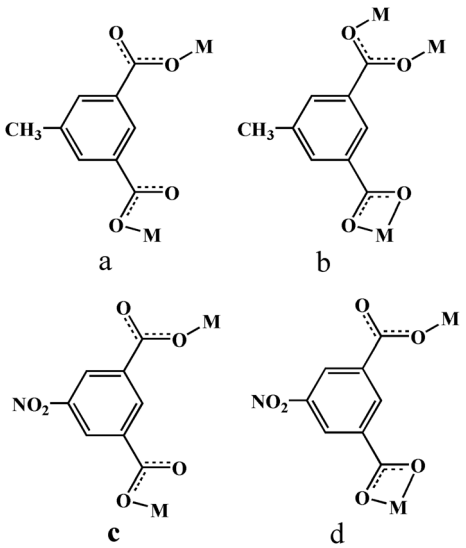

Scheme 1 Coordination modes of the aromatic dicarboxylic acids in 1–4.

binuclear node are further bridged by two bpp ligands with the two pyridyl groups almost parallel to each other (dihedral angle between the two pyridyl groups is *ca.* 16.43°). These binuclear subunits are further linked by mip^{2-} anion to form one-dimensional chain structure (Fig. 2b). Packing of these chains results in a 3D supramolecular structure as shown in Fig. 2c. The dihedral angle in **2** is much smaller than that in **1** due to the two flexible C–C single bonds between the two pyridyl groups. This long distance makes it much more flexible so as to show different configurations and resulting different structures.

Crystal structure of 3

Single crystal X-ray diffraction reveals that complex **3** crystallize in $P\bar{1}$ space group of the triclinic system. The asymmetric unit of **3** consists of two Zn(II) ions, two bpp ligands and two fully deprotonated nip^{2-} ligands. Both the local coordination environments around Zn1 and Zn2 can be described as slightly distorted tetrahedron geometry with two carboxylate oxygen atoms from two nip^{2-} ligands and two pyridyl nitrogen atoms

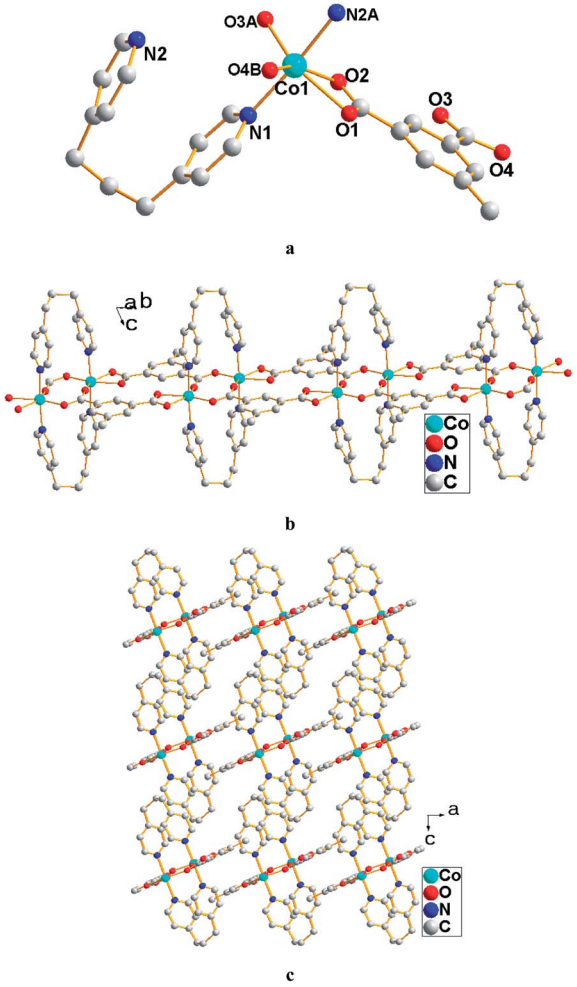

Fig. 2 (a) The coordination environment of Co(II) ion in **2**; (b) view of a single chain and (c) packing of the 1D chains in complex **2**.

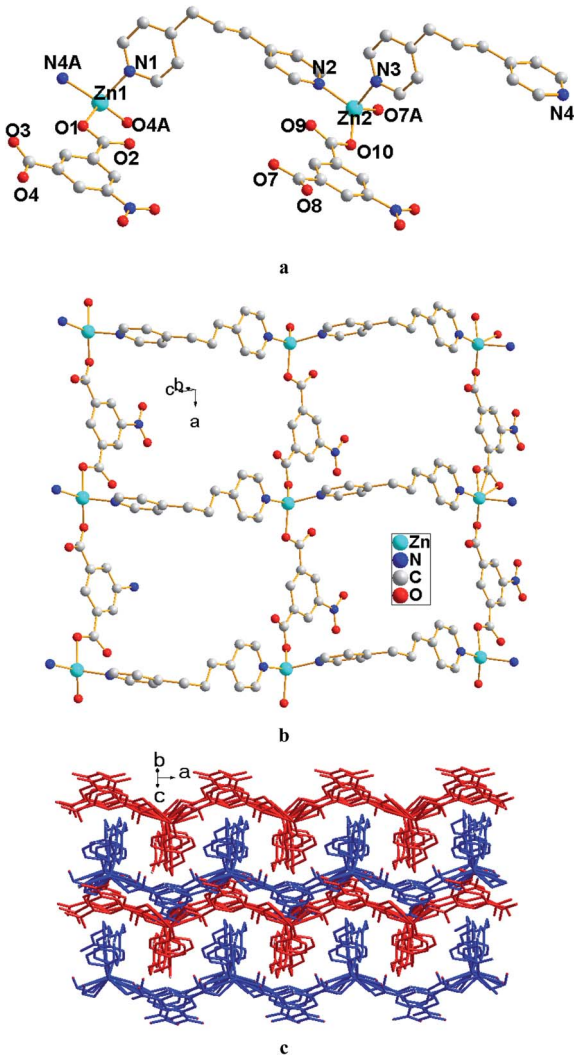

Fig. 3 (a) The coordination environment of Zn(II) ion in **3**; (b) a view of the 2D 4^4-sql layer and (c) packing of the 2D layers in *ABAB* mode.

from two bpp molecules as shown in Fig. 3a. The Zn–N bond distance ranges from 2.046(4) to 2.051(4) Å while the Zn–O bond length ranges from 1.959(3) to 1.961(3) Å, respectively, which are well-matched to those observed in other zinc–nitrogen and zinc–oxygen donor compounds.[16,17] The nip^{2-} ligands show η^1–η^1 coordination mode as shown in Scheme 1c linking the central Zn(II) ions into chain structure, which are further bridged by the bpp ligand into 2D corrugated layer structure with 4^4-sql topology as shown in Fig. 3b and c. Packing of such layers in *ABAB* mode form the whole structure of compound **3** (Fig. 3c). These layers are further stabilized by π···π interactions between the layers to form a 3D supramolecular structure.

Crystal structure of 4

Complex **4** crystallizes in a monoclinic space group *C*2/*c*. Its asymmetric unit contains one independent Co(II) cation, one bpp molecules and one nip^{2-} anion. As shown in Fig. 1a, the coordination number of Co(II) ion is six and each Co(II) is linked to three oxygen atoms from two nip^{2-} anion with the Co–O bond distance range from 2.031(4) Å to 2.247(4) Å, two nitrogen atoms from two bpp ligands with bond length of Co1–N1 = 2.143(5) Å, Co1–N2A = 2.122(5) Å and one ligated water molecule with the Co1–O1W bond length of 2.102(5) Å. These values are comparable to those in reported Co compounds.[18,19] The nip^{2-} anion acts in a η^2–η^1 coordination mode as shown in Scheme 1d with one of the two carboxylate groups adopts chelating coordination mode while the other one acts in a monodentate bridging mode. The bpp ligand exhibits a dihedral angle of 81.77° between the two pyridyl planes in complex **4**. This means that the two pyridyl planes of a bpp ligand are almost perpendicular to each other, which is further validated as the ligand link the Co(II) ions into 1D zigzag chains. Meanwhile, the Co(II) ions are also linked by the H_2nip ligand into 1D chains and the two kinds of chains intersect with each other to give up a 3D diamond network (Fig. 4b). Then the adamantanoid cage also shows a large cavity as that in compound **1**, which is interpenetrated by another independent framework to form a 3D doubly interpenetrating structure as shown in Fig. 4c.

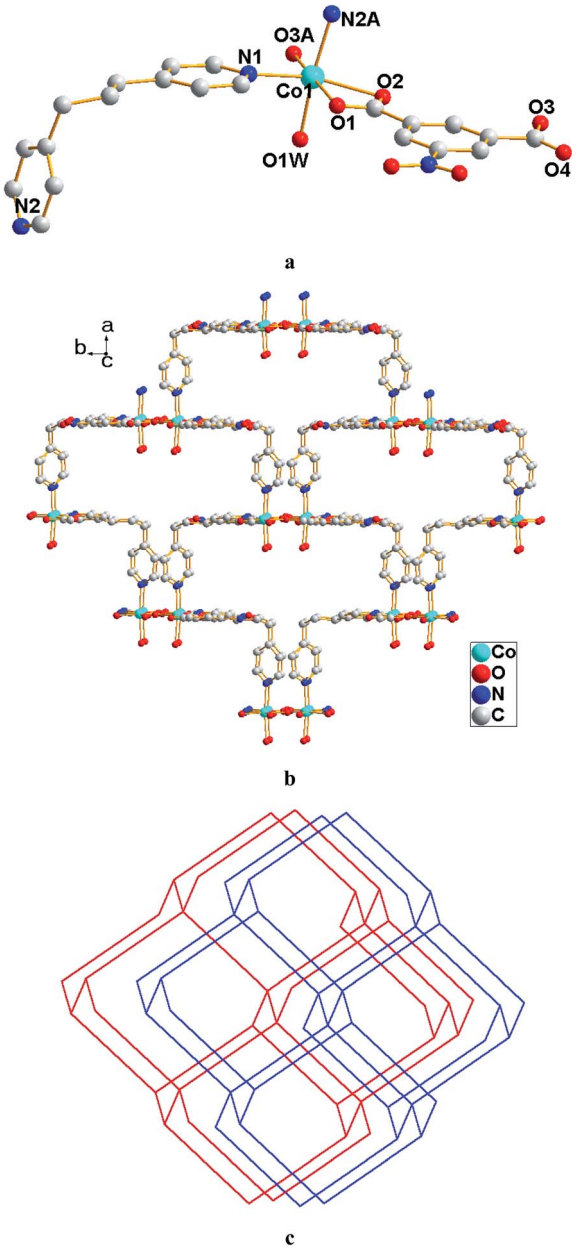

Fig. 4 (a) The coordination environment of Co(II) ion in **4**; (b) view of the 3D *dia* network and (c) schematic illustration of the two-fold interpenetrating network in **4**.

Structure discussion

Coordination modes of the two aromatic dicarboxylic acids are shown in Scheme 1 and dihedral angles between the two pyridyl groups of the bpp ligand in complexes **1–4** are listed in Table 2. The different coordination modes and dihedral angles indicate that mixed N-coordinated ligand and polycarboxylate ligand systems can surely provide various possibilities for the construction of coordination polymers with distinct structure features. As shown in Table 2, for the two Zn(II)-based complexes **1** and **3**, H_2mip and H_2nip hold the same η^1–η^1 coordination mode with all the carboxylate group acting in a monodentate bridging mode. While for the two Co(II)-based complexes **2** and **4**, H_2mip and H_2nip hold similar bidentate linking mode. That is to say it's the central metal cations that greatly affect the coordination mode of the aromatic dicarboxylic acids in our system. Undoubtedly, such different coordination modes of ligands can significantly influence the topological networks of coordination complexes. On the other hand, the two C–C single bands between the two pyridyl groups in the bpp ligand give it sufficient flexibility to show different configurations with various dihedral angles when coordination in different environment as in complexes **1–4**. Synthesis of coordination complexes with interesting structures and novel properties based on mixed N-coordinated ligand and polycarboxylate ligand system is now a current research focus for chemists. Some other interesting networks assemble from 1,3-bis-(4-pyridyl)-propane and aromatic acids have also been reported.[20] For example, Liu and co-workers reported a novel 3D coordination polymer with (10,3)-d topology left/right-handed

Table 2 The ligand conformations and the corresponding angles for 1–4

Complexes	Metal centers	Dihedral angles of bpp	Coordination modes of carboxylic acids	Structures
1	Zn	75.76°	η^1–η^1	Fourfold *dia* interpenetration
3	Zn	88.10°	η^1–η^1	4^4-sql layer
2	Co	16.43°	$\eta^2\mu_2$–η^2	Chain
4	Co	81.77°	η^2–η^1	Twofold *dia* interpenetration

helical channels based on mixed ligands of 5-sulfoisophthalate and bpp.[20a] Li and co-workers reported a complex with 3-fold interpenetrating *dia* network and interesting nonlinear-optic property assemble from 2-amino-1,4-benzene dicarboxylic acid and bpp.[20b] Among these structures, two-fold interpenetrating frameworks are most common while those four-fold interpenetrating networks are relative rare and somewhat uncommon.

Thermal analysis and PXRD results

Thermogravimetric analysis (TGA) studies were performed to characterize the thermal stability of complexes **1–4** under an nitrogen atmosphere. The TGA curves of complexes **1–3** (Fig. S2†) show no weight loss below 300 °C as there is no water or other solvent molecule in the structure. One obvious weight loss began at about 315 °C indicating the decomposition of the framework. Complex **4** exhibits two significant weight losses. The first weight loss of 3.79% occurs between 120 °C and 177 °C corresponds to the removal of the one coordinated water molecule (calcd: 3.72%). And then begin to decompose from 245 °C upon further heating. Additionally, to confirm whether the crystal structures of **1–4** are truly representative of the bulk materials, powder X-ray diffraction has been performed with the as-synthesized polycrystalline samples under room temperature. The results shown in Fig. S1† indicate that the X-ray powder diffraction data are in agreement with that calculated on the basis of the single crystal structural datas, that is, **1–4** have been obtained successfully as pure crystalline phases.

FT-IR spectra

The FT-IR spectra of complexes **1–4** were determined in the frequency range of 500–4000 cm^{-1}, as shown in Fig. S3.† The strong peaks around 1624 and 1430 cm^{-1} for **1**, 1616 and 1427 cm^{-1} for **2**, 1643 and 1434 cm^{-1} for **3** and 1630 and 1429 cm^{-1} for **4** are associated with the asymmetric and symmetric stretching vibrations of carboxylate groups.[15] The bands around 1334 and 1031 cm^{-1} for **1**, 1389 and 1050 cm^{-1} for **2**, 1337 and 1073 cm^{-1} for **3** and 1367 and 1072 cm^{-1} for **4** are characteristic of the stretching vibrations of C–N bond, suggesting the presence of the pyridyl ring.[21]

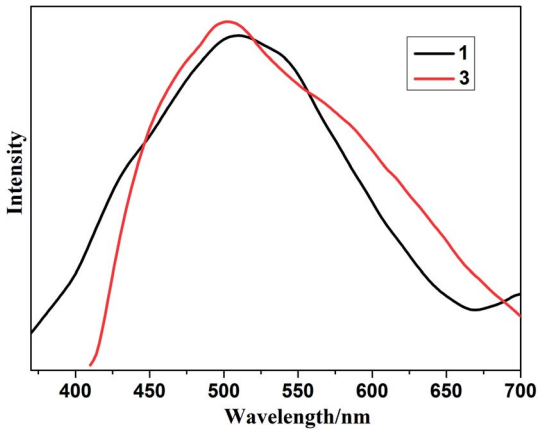

Fig. 5 Luminescent spectra of compounds **1** and **3**.

UV-vis absorbance properties and photoluminescent properties

The solid-state UV-vis spectra of compounds **1–4** are measured and the results are shown in Fig. S4.† Compounds **1–4** show similar weak absorption band with maximum at about 330 nm, which is probably owing to n → π* transitions of the aromatic rings. Considering the excellent luminescence of coordination polymers constructed from d^{10} metal ions, the solid-state luminescent properties of compounds **1** and **3** have been investigated at room temperature. As depicted in Fig. 5, Complexes **1** and **3** exhibit broad emission bands with maximum at 502 and 510 nm upon excitation at 330 nm respectively. Luminescent spectra of the bpp, H_2mip and H_2nip have also been investigated but no emission band has been observed in the range of 450 to 600 nm upon excitation at 330 nm. The H_2mip ligand display a emission peak at 357 nm upon excitation at 315 nm according to literature.[22] These results indicate that the emissions of compounds **1** and **3** can be probably ascribed to metal-to-ligand charge transfer (MLCT) transition between Zn(II) ions and the aromatic ligands.[23,24] As for complexes **2** and **4**, Co^{2+} ion has unsaturated electron configuration d^7, the interaction between Co^{2+} ion and ligand leads to strong quenching effect and therefore the two compounds don't exhibit the emission nature.

Magnetic property

The variable-temperature magnetic susceptibility study of complex **2** and **4** were carried out at an applied field of 1000 Oe in the temperature range of 2–300 K, as shown in Fig. 6. For complex **2**, the $\chi_m T$ value at 300 K is *ca.* 3.87 cm^3 K mol^{-1}, which is slightly higher than that of the spin-only value of 3.75 cm^3 K mol^{-1} for two Co(II) ions with $S = 3/2$ and $g = 2$ owing to the significant orbital contribution of Co(II) in an octahedral environment.[25,26] The $\chi_m T$ value decreases gradually upon lowering the temperature and goes down to a minimum of 1.80 cm^3 K mol^{-1} at 2 K. The temperature dependence of the reciprocal susceptibility above 35 K obeys the Curie–Weiss law with a Weiss constant, $\theta = -16.12$ K and a Curie constant, $C_m = 4.04$ cm^3 mol^{-1} K. The high value of C and negative θ value may be

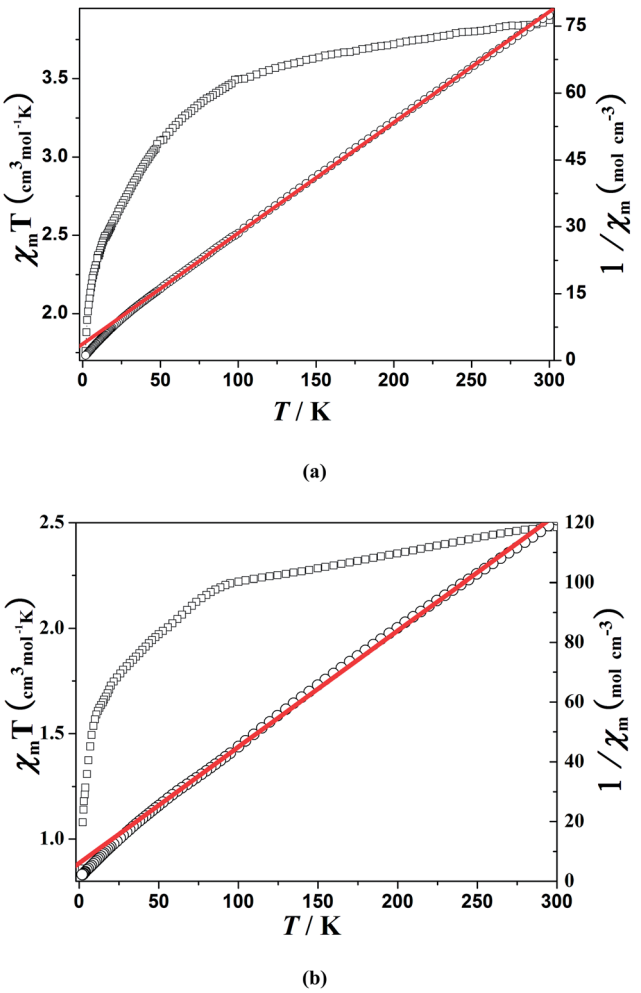

Fig. 6 Plots of experimental $\chi_m T$ *vs.* T (□) and $1/\chi_m$ *vs.* T (○) for **2** (a) and **4** (b). The solid red line shows the Curie–Weiss fitting.

due to the spin-orbit coupling, which is remarkable for the $^4T_{1g}$ state of Co(II) in an octahedral ligand field.[27] These results clearly indicate that weak antiferromagnetic coupling interactions exist between Co(II) ions in compound **2**. For complex **4**, the $\chi_m T$ value is 2.48 cm^3 K mol^{-1} at 300 K, which is larger than the spin-only value of a single Co(II) ion and decreases upon cooling to 0.76 cm^3 K mol^{-1} at 2 K. The temperature dependence of the reciprocal susceptibility above 40 K obeys the Curie–Weiss law with a Weiss constant, $\theta = -20.15$ K and a Curie constant, $C_m = 2.95$ cm^3 mol^{-1} K. The high value of C and negative θ value indicate that antiferromagnetic coupling interactions exist between Co(II) ions in compound **4**. As the large distance of 8.78 Å between Co(II) ions within one *dia* subunit, we conclude that the coupling interactions may be mainly originate from Co(II) ions from different *dia* subunits as the nearest inter-net distance between Co(II) ions is 5.23 Å.[28]

Conclusion

In summary, four new complexes have been successfully synthesized under hydrothermal condition. Due to the flexibility and configuration of the bpp ligand and the different coordination modes of the H_2mip or H_2nip ligands, the four complexes show different structures: fourfold 3D interpenetrating framework with *dia* topology for **1**, 3D supramolecular structure assembled from binuclear chains for **2**, 3D supramolecular structure based on 2D sql layers packing of *ABAB* mode for **3** and 3D doubly interpenetrating diamond network for **4**. The results indicate that the flexibility and the configuration of ligands play a crucial role in determining the topological structure of the resulting coordination polymers. The photoluminescent properties of **1** and **3** were investigated, which were assigned to MLCT transitions. The magnetic property studies of **2** and **4** indicating antiferromagnetic coupling interactions exist between Co(II) ions.

Acknowledgements

This work was financially supported by The Shandong Provincial Natural Science Foundation of China (grant no. ZR2012BQ004) and Doctor's Foundation of University of Jinan (XBS1208), C. Li, as a Taishan Scholar Endowed Professor, acknowledges the support from Shandong Province and UJN.

References

1 (*a*) M. O'Keeffe and O. M. Yaghi, *Chem. Rev.*, 2012, **112**, 675; (*b*) M. Eddaoudi, D. B. Moler, H. Li, B. Chen, T. M. Reineke, M. O'Keeffe and O. M. Yaghi, *Acc. Chem. Res.*, 2001, **34**, 319; (*c*) J. R. Li, R. J. Kuppler and H. C. Zhou, *Chem. Soc. Rev.*, 2009, **38**, 1477; (*d*) S. Kitagawa, R. Kitaura and S. Noro, *Angew. Chem., Int. Ed.*, 2004, **43**, 2334.

2 (*a*) E. Coronado and G. M. Espallargas, *Chem. Soc. Rev.*, 2013, **42**, 1525; (*b*) Y. Cui, Y. Yue, G. Qian and B. Chen, *Chem. Rev.*, 2012, **112**, 1126; (*c*) J. P. Zhang, Y. B. Zhang, J. B. Lin and X. M. Chen, *Chem. Rev.*, 2012, **112**, 1001; (*d*) T. Panda, P. Pachfule, Y. Chen, J. Jiang and R. Banerjee, *Chem. Commun.*, 2011, **47**, 2011; (*e*) M. F. Wu, M. S. Wang, S. P. Guo, F. K. Zheng, H. F. Chen, X. M. Jiang, G. N. Liu, G. C. Guo and J. S. Huang, *Cryst. Growth Des.*, 2011, **11**, 372.

3 (*a*) C. W. Hu, T. Sato, J. Zhang, S. Moriyama and M. Higuchi, *J. Mater. Chem. C*, 2013, **1**, 3408; (*b*) S. S. Kaye and J. R. Long, *J. Am. Chem. Soc.*, 2008, **130**, 806; (*c*) P. H. Guo, J. L. Liu, J. H. Jia, J. Wang, F. S. Guo, Y. C. Chen, W. Q. Lin, J. D. Leng, D. H. Bao, X. D. Zhang, J. H. Luo and M. L. Tong, *Chem.–Eur. J.*, 2013, **19**, 8769; (*d*) F. N. Dai, H. Y. He and D. F. Sun, *J. Am. Chem. Soc.*, 2008, **130**, 14064.

4 (*a*) S. S. Nagarkar, B. Joarder, A. K. Chaudhari, S. Mukherjee and S. K. Ghosh, *Angew. Chem., Int. Ed.*, 2013, **52**, 2881; (*b*) X. L. Wang, C. Qin, S. X. Wu, K. Z. Shao, Y. Q. Lan, S. Wang, D. X. Zhu, Z. M. Su and E. B. Wang, *Angew. Chem., Int. Ed.*, 2009, **48**, 5291; (*c*) S. T. Zheng, T. Wu, B. Irfanoglu, F. Zuo, P. Y. Feng and X. H. Bu, *Angew. Chem., Int. Ed.*, 2011, **50**, 8034.

5 (*a*) D. Sun, Z. H. Yan, V. A. Blatov, L. Wang and D. F. Sun, *Cryst. Growth Des.*, 2013, **13**, 1277; (*b*) H. Wu, J. Yang, Y. Y. Liu and J. F. Ma, *Cryst. Growth Des.*, 2012, **12**, 2272; (*c*) C. P. Li and M. Du, *Chem. Commun.*, 2011, **47**, 5958; (*d*)

D. Liu, Z. G. Ren, H. X. Li, Y. Chen, J. Wang, Y. Zhang and J. P. Lang, *CrystEngComm*, 2010, **12**, 1912.

6 (*a*) B. Li, L. Q. Chen, R. J. Wei, J. Tao, R. B. Huang, L. S. Zheng and Z. P. Zheng, *Inorg. Chem.*, 2011, **50**, 424; (*b*) Q. Liu, L. N. Jin and W. Y. Sun, *Chem. Commun.*, 2012, **48**, 8814; (*c*) W. G. Lu, L. Jiang and T. B. Lu, *Cryst. Growth Des.*, 2010, **10**, 4310.

7 (*a*) Y. H. Wang, K. L. Chu, H. C. Chen, C. W. Yeh, Z. K. Chan, M. C. Suen and J. D. Chen, *CrystEngComm*, 2006, **8**, 84; (*b*) M. Maekawa, T. Tominaga, K. Sugimoto, T. Okubo, T. K. Sowa, M. Munakata and S. Kitagawa, *CrystEngComm*, 2012, **14**, 1345; (*c*) W. H. Huang, X. J. Luan, X. Zhou, J. Chen, Y. Y. Wang and Q. Z. Shi, *CrystEngComm*, 2013, **15**, 10389.

8 (*a*) B. Xu, X. Lin, Z. Z. He, Z. J. Lin and R. Cao, *Chem. Commun.*, 2011, **47**, 3766; (*b*) B. Xu, J. Lü and R. Cao, *Cryst. Growth Des.*, 2009, **9**, 3003; (*c*) B. Xu, Z. J. Lin, L. W. Han and R. Cao, *CrystEngComm*, 2011, **13**, 440; (*d*) B. Xu, G. L. Li, H. X. Yang, S. Y. Gao and R. Cao, *Inorg. Chem. Commun.*, 2011, **14**, 493.

9 (*a*) M. H. Yu, M. Hu and Z. T. Wu, *RSC Adv.*, 2013, **3**, 25175; (*b*) Y. F. Wang, Z. Li, Y. C. Sun, J. S. Zhao and L. Y. Wang, *CrystEngComm*, 2013, **15**, 9980; (*c*) Z. X. Kang, M. Xue, L. L. Fan, J. Y. Ding, L. J. Guo, L. X. Gao and S. L. Qiu, *Chem. Commun.*, 2013, **49**, 10569.

10 (*a*) J. Y. Gao, N. Wang, X. H. Xiong, C. J. Chen, W. P. Xie, X. R. Ran, Y. Long, S. T. Yue and Y. L. Liu, *CrystEngComm*, 2013, **15**, 3261; (*b*) L. Hou, L. N. Jia, W. J. Shi, L. Y. Du, J. Li, Y. Y. Wang and Q. Z. Shi, *Dalton Trans.*, 2013, **42**, 6306.

11 (*a*) B. Liu, M. Tu, D. Zacher and R. A. Fischer, *Adv. Funct. Mater.*, 2013, **23**, 3790; (*b*) K. Jayaramulu, N. Kumar, A. Hazra, T. K. Maji and C. N. R. Rao, *Chem.–Eur. J.*, 2013, **19**, 6966; (*c*) Z. An, J. Gao and L. Zhu, *J. Mol. Struct.*, 2013, **1054–1055**, 234.

12 *Oxford Diffraction, CrysAlisPro, Version 1.171.33.55*, Oxford Diffraction Ltd., Yarnton, Oxfordshire, 2010.

13 G. M. Sheldrick, *SADABS, Siemens Area Detector Absorption Correction Program*, University of Göttingen, Göttingen, Germany, 1994

14 G. M. Sheldrick, *SHELXS-97, Program for Crystal Structure Solution and Refinement*, University of Göttingen, 1997.

15 V. A. Blatov, *IUCr, Comput. Comm. Newslett.*, 2006, **7**, 4, see also http://www.topos.ssu.samara.ru.

16 (*a*) H. M. He, F. X. Sun, H. M. Su, J. T. Jia, Q. Li and G. S. Zhu, *CrystEngComm*, 2014, **16**, 339; (*b*) I. P. Oliveri, S. Fsilla, A. Colombo, C. Dragonetti, S. Righetto and S. Bella, *Dalton Trans.*, 2014, **43**, 2168.

17 (*a*) D. Dey, S. Roy, R. D. Purkayastha, R. Pallepogu and P. McArdle, *J. Mol. Struct.*, 2013, **1053**, 127; (*b*) L. Xu, E. Y. Choi and Y. U. Kwon, *Inorg. Chem. Commun.*, 2008, **11**, 150.

18 (*a*) L. L. Zheng, J. D. Leng, R. Herchel, Y. H. Lan, A. K. Powell and M. L. Tong, *Eur. J. Inorg. Chem.*, 2010, 2229; (*b*) L. Qin, L. N. Wang, P. J. Ma and G. H. Cui, *J. Mol. Struct.*, 2014, **1059**, 202.

19 (*a*) Y. Q. Wang, W. W. Sun, Z. D. Wang, Q. X. Jia, E. Q. Gao and Y. Song, *Chem. Commun.*, 2011, **47**, 6368; (*b*) Y. Yuan, D. Wang, S. X. Liu, Y. Wang, J. Y. Liu, B. Ding and X. J. Zhao, *Inorg. Chim. Acta*, 2013, **407**, 239.

20 (*a*) Q. Y. Liu, Y. L. Wang, Z. M. Shan, R. Cao, Y. L. Jiang, Z. J. Wang and E. L. Yang, *Inorg. Chem.*, 2010, **49**, 8191; (*b*) L. L. Wen, L. Zhou, B. G. Zhang, X. G. Meng, H. Qu and D. F. Li, *J. Mater. Chem.*, 2012, **22**, 22603; (*c*) H. Q. Hao, H. S. Li and M. X. Peng, *Inorg. Chem. Commun.*, 2012, **22**, 6.

21 P. S. Kalsi, *Spectroscopy Of Organic Compounds*, New Age International, New Delhi, 2008.

22 Q. B. Bo, H. Y. Wang, D. Q. Wang, Z. W. Zhang, J. L. Miao and G. X. Sun, *Inorg. Chem.*, 2011, **50**, 10163.

23 (*a*) M. D. Allendorf, C. A. Bauer, R. K. Bhakta and R. J. T. Houk, *Chem. Soc. Rev.*, 2009, **38**, 1330; (*b*) M. P. Suh, Y. E. Cheon and E. Y. Lee, *Coord. Chem. Rev.*, 2008, **252**, 1007; (*c*) M. Frisch and C. L. Cahill, *Dalton Trans.*, 2005, 1518.

24 (*a*) C. Q. Jiao, C. Y. Huang, Z. G. Sun, K. Chen, C. L. Wang, C. Li, Y. Y. Zhu, H. Tian, S. H. Sun, W. Chu and M. J. Zheng, *Inorg. Chem. Commun.*, 2012, **17**, 64; (*b*) B. L. Chen, L. B. Wang, F. Zapata, G. D. Qian and E. B. Lobkovsky, *J. Am. Chem. Soc.*, 2008, **130**, 6718.

25 (*a*) O. Kahn, *Molecular Magnetism*, VCH Publishers, New York, 1993; (*b*) R. Y. Li, X. Y. Wang, T. Liu, H. B. Xu, F. Zhao, Z. M. Wang and S. Gao, *Inorg. Chem.*, 2008, **47**, 8134.

26 (*a*) M. Clemente-León, E. Coronado, C. Martí-Gastaldo and F. M. Romero, *Chem. Soc. Rev.*, 2011, **40**, 473; (*b*) Y. Chen, Y. Song, Y. Zhang and J. P. Lang, *Inorg. Chem. Commun.*, 2008, **11**, 572.

27 (*a*) B. N. Figgis and M. A. Hitchman, *Ligand Field Theory and Its Applications*, Wiley-VCH, 2000; (*b*) E. Coronado, J. R. Galán-Mascarós and C. Martí-Gastaldo, *J. Am. Chem. Soc.*, 2008, **130**, 14987; (*c*) Q. Chu, G. X. Liu, T. Okamura, Y. Q. Huang, W. Y. Sun and N. Ueyama, *Polyhedron*, 2008, **27**, 812.

28 (*a*) A. M. P. Peedikakkal, Y. M. Song, R. G. Xiong, S. Gao and J. J. Vittal, *Eur. J. Inorg. Chem.*, 2010, 3856; (*b*) D. Gatteschi and R. Sessoli, *Angew. Chem., Int. Ed.*, 2003, **42**, 268.

